Normal Form Analysis of Chua's Circuit with Applications for Trajectory Recognition

Edward J. Altman, *Member, IEEE*

Abstract—**Nonlinear analysis techniques are applied to Chua's circuit equations in which the piecewise-linear characteristic is replaced by a cubic nonlinearity. Center manifold theory is used to derive a reduced order expression for Chua's circuit near the equilibria. Normal form theory is applied to simplify the form of the dynamics on the center manifold. Closed-form expressions for the normal form coefficients are obtained in terms of the dynamics on the center manifold. A one parameter bifurcation function is derived from the normal form expression that describes the amplitude of stable limit cycles transverse to the Hopf bifurcation curve. The results of the analysis are illustrated by an array of Chua's circuits used for trajectory recognition.**

I. Introduction

TRADITIONAL hand gesture recognition methods rely on the frame-by-frame analysis of a sequence of images to determine the motion trajectory of the hand. Recognition is typically accomplished by matching the space curve of the input trajectory to a set of reference space curves. Additionally, hand gestures exhibit considerable variation in the shape of the space curve and the speed of the motion. Consequently, a class of motion trajectories must be associated with a single gesture, thus further complicating the recognition problem. An alternative approach, which accounts for the variation among gestures, is to view each class of trajectories as motions constrained to a manifold surface in 3-D space. Similarly, nonlinear dynamical systems evolve with time along stable manifold surfaces according to a set of rules expressed as differential equations. By a suitable mapping of the input trajectory onto the dynamical system, the recognition of a motion trajectory as a member of a particular class reduces to the identification of the corresponding manifold surface as both trajectories evolve over time. The fundamental detection problem concerns the use of motion trajectories from hand gestures to drive the dynamical system onto an attracting surface.

In this paper, center manifold theory and normal form theory are used to relate the local behavior of Chua's circuit to the input trajectory to be recognized. The relative simplicity of Chua's circuit and the ability to generate a large variety of behaviors in this single circuit motivate the choice of this system [1]. The piecewise-linear characteristic is replaced with a cubic nonlinearity in order to apply the formal methods of nonlinear analysis. The analysis procedures are based on diffeomorphisms (smooth, invertible transformations), and therefore, the inverse transformations can be used for the design of new dynamics from the center manifold or normal form representations.

Manuscript received April 18, 1993; revised May 26, 1993.

The author is with ATR Communication Systems Research Laboratories, Kyoto, Japan.

IEEE Log Number 9211627.

The real-time recognition of motion trajectories for hand gestures relies on the use of the hand position as a function of time to drive the dynamical system toward an attracting surface. Chua's circuit is known to undergo a series of bifurcations from fixed points, to limit cycles, to a cascade of period doubling oscillations leading to chaotic oscillations in the vicinity of the center manifold [1], [2]. The rapid entrainment of the chaotic system to an external signal having a trajectory near the center manifold surface provides the basic mechanism for trajectory recognition.

The recognition of many trajectories requires the use of many dynamical systems. When these systems are arranged in a 2-D array, then the variation of responses to the common input trajectory creates a spatial pattern. This spatial pattern is subsequently used to recognize the input trajectory. The significance of this approach is that the recognition of multiple, complex trajectories is reduced to the problem of recognizing static patterns generated by the array.

The use of chaotic oscillations for the recognition of hand motion trajectories is motivated by several factors. First, the stable states of linear systems have only fixed point or periodic orbits, whereas nonlinear systems can have quasi-stable states that are surfaces (which are also called attractors or stable manifolds). Thus, nonlinear systems are useful for recognizing families of trajectories occurring on surfaces in 3-D space. Second, chaotic systems are highly responsive to external inputs, thus providing rapid entrainment to the driving signal. Finally, chaotic systems are able to rapidly move from one region of the state space to another. We envision that this property will be useful for detecting when one motion trajectory ends and a new trajectory begins in the recognition of continuous gestures in sign language.

Recent advances in the analysis of Chua's circuit as a nonlinear oscillator provide a mathematical basis for the design and application of dynamical systems [3]. An additional motivating factor for the use of Chua's circuit equations as a model dynamical system is that it has recently become possible to implement this circuit entirely in CMOS [4]. Thus, large-scale production of this circuit is now possible.

The organization of this paper is as follows. The nonlinear analysis of Chua's circuit is presented in Section II. The derivation of the center manifold surface and the computation of the normal form using Ushiki's method are presented in detail. Closed-form expressions for the normal form coeffi-

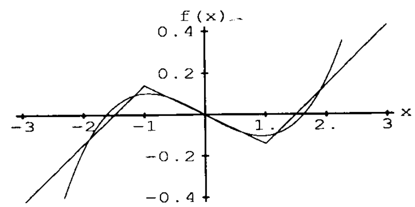

Fig. 1. Cubic nonlinearity of Chua's circuit equations.

cients in terms of the dynamics on the center manifold are also given. In Section III, a 1-D bifurcation function describing the amplitude of limit cycle oscillations is derived from the normal form expression. The preliminary results for the application of this theory for real-time hand gesture recognition are discussed in Section IV.

II. Normal Form Computation

In the study of the local behavior of solutions of nonlinear differential equations, the choice of coordinate systems plays a major role in identifying the qualitative properties of the flows. The *normal form* is considered as the simplest member of an equivalence class of vector fields, all exhibiting the same qualitative behavior near the equilibria of the system. The basic approach to constructing the normal form equations for a dynamical system is based on the computation of nonlinear transformations that systematically reduce the coupling among low-order terms in the original dynamical system. Recently, Ushiki has introduced the use of *infinitesimal deformations* to incrementally transform the vector field into a normal form with the fewest possible coefficients [5]–[7].

2.1. The Dynamics

Bifurcation theory is applied in this paper to analyze the dimensionless form of Chua's circuit equations [8]–[11]

$$\begin{aligned} \dot{x} &= \alpha[y - f(x)] \\ \dot{y} &= x - y + z \\ \dot{z} &= -\beta y \end{aligned} \tag{1}$$

where

$$f(x) = (m_1 + 1)x + \frac{1}{2}(m_0 - m_1)[|x+1| - |x-1|]. \tag{2}$$

In most previous analysis, the parameters are fixed with the values $m_0 = -\frac{8}{7}$ and $m_1 = -\frac{5}{7}$, and (1) is treated as a two-parameter dynamical system with α and β as bifurcation parameters. In this paper, we examine the case where $f(x)$ is a cubic function

$$f(x) = c_0 x + c_1 x^3 \tag{3}$$

in which a least squares approximation to (2) yields $c_0 = -\frac{1}{6}$ and $c_1 = \frac{1}{16}$. The shape of the cubic nonlinearity of $f(x)$ is illustrated in Fig. 1.

The first-order normal form concides with the Jordan normal form at an equilibrium point. Chua's circuit has three equilibria at $P_0 = (0,0,0)$ and $P_\pm = \left(\pm\sqrt{-\frac{1+c_0}{c_1}}, 0, \mp\sqrt{-\frac{1+c_0}{c_1}}\right)$. Near the equilibrium P_+, we have the linearization

$$M = Df|_{P_+} = \begin{bmatrix} \alpha c_0 - 3(c_0+1) & \alpha & 0 \\ 1 & -1 & 1 \\ 0 & -\beta & 0 \end{bmatrix}. \tag{4}$$

If α and β are chosen such that (4) has a pair of complex conjugate eigenvalues $\sigma \pm i\omega_0$ and a real eigenvalue γ, then the Jordan form

$$\begin{bmatrix} \dot{u} \\ \dot{v} \\ \dot{w} \end{bmatrix} = \begin{bmatrix} \sigma & -\omega_0 & 0 \\ \omega_0 & \sigma & 0 \\ 0 & 0 & \gamma \end{bmatrix} \begin{bmatrix} u \\ v \\ w \end{bmatrix} + \begin{bmatrix} f(u,v,w) \\ g(u,v,w) \\ h(u,v,w) \end{bmatrix} \tag{5}$$

has the linear part in block diagonal form and the higher order nonlinear terms are expressed by the functions $f(\cdot)$, $g(\cdot)$, and $h(\cdot)$ [12].

2.2. Transformation Theory

The equilibrium of the vector field is said to be *hyperbolic*, if it does not contain any eigenvalues with zero real part. According to the *Hartman-Grobman theorem* [13] the vector field near a hyperbolic equilibrium can be accurately characterized by its linearization. In order to study the Hopf bifurcation near $\sigma = 0$, it is convenient to treat σ as an additional variable and study the effect of variations in this new variable. The augmented system now has both *central eigenvalues*, which lie on the imaginary axis in the complex plane, and noncentral eigenvalues with nonzero real part. A systematic method for constructing a reduced order vector field by eliminating the noncentral eigenvalues is provided by the *center manifold theorem* [13], [14]. This vector field consist of an invariant manifold called the *center manifold*, which is tangent to the center eigenspace at the equilibrium of the system.

The computation of the second-order normal form assumes that the equilibrium has been translated to the origin. The normal form computation requires that the dynamics be projected onto a reduced dimensional space called the center manifold. The basic idea for calculating the center manifold is to find a nonlinear projection of the original state space onto a reduced space where the complicated dynamics occurs [13], [15]. We seek a lower dimensional approximation for the Jordan form of the model dynamics expressed by (5). In order to examine Hopf bifurcation phenomena in this system, we create a suspended system [13], [15]

$$\begin{bmatrix} \dot{u} \\ \dot{v} \\ \dot{\sigma} \\ \dot{w} \end{bmatrix} = \begin{bmatrix} 0 & -\omega_0 & 0 & 0 \\ \omega_0 & 0 & 0 & 0 \\ 0 & 0 & 0 & 0 \\ 0 & 0 & 0 & \gamma \end{bmatrix} \begin{bmatrix} u \\ v \\ \sigma \\ w \end{bmatrix} + \begin{bmatrix} \sigma u \\ \sigma v \\ 0 \\ 0 \end{bmatrix} + \begin{bmatrix} f(u,v,w) \\ g(u,v,w) \\ 0 \\ h(u,v,w) \end{bmatrix} \tag{6}$$

by treating σ as an additional variable with the condition $\dot{\sigma} = 0$. The term σ is the real part of the complex conjugate pair of eigenvalues of the Jordan form that will later serve as a bifurcation parameter.

The surface of the center manifold is described locally by the nonlinear graph [16]

$$w = S(u, v, \sigma). \tag{7}$$

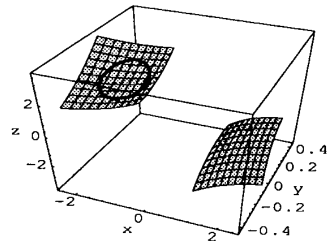

Fig. 2. Center manifolds at $P_{\pm}$ with limit cycle oscillations on the manifold surface.

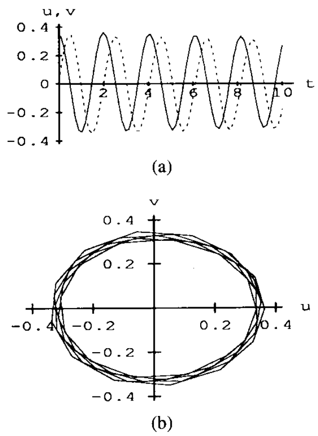

Fig. 3. Limit cycle oscillations of Chua's circuit in the reduced-order space of the center manifold. (a) Temporal profiles of the center manifold variables u (solid) and v (dashed). (b) Phase plot in the uv space.

A view of the two center manifolds associated with P_+ and P_- projected back into the xyz coordinates of Chua's circuit is illustrated in Fig. 2. The limit cycle oscillations of Chua's circuit in the uv coordinates of the center manifold in Fig. 3 show that the complex limit cycle trajectories in the xyz space have a simple form in the uv coordinate space of the center manifold.

All of the above transformations are diffeomorphisms (smooth, invertable maps), and therefore, the local dynamics near the equilibria of the original system are topologically equivalent to the dynamics on the center manifold. Since the trajectories of the original system converge to trajectories on the center manifold surface, the behavior of the system can be modified by reshaping the center manifold surface and transforming back to the original coordinates. The projection of the dynamics onto the center manifold provides a mechanism for modifying the vector field to optimize the response of the system to the input trajectory to be recognized.

If the dynamics on the center manifold is stable, then the trajectories on the manifold are related to trajectories in the first order normal form (Jordan form) in (5) by

$$\begin{aligned} x(t) &= u(t) + \mathcal{O}(e^{-\gamma t}) \\ y(t) &= v(t) + \mathcal{O}(e^{-\gamma t}) \\ z(t) &= S(u(t), v(t), \sigma) + \mathcal{O}(e^{-\gamma t}) \end{aligned} \tag{8}$$

where $\gamma > 0$[14], [15].

2.3. Ushiki's Normal Form

In the remainder of this section, we summarize Ushiki's refinement of Takens' normal form computation for nonlinear vector fields [5]–[7]. Here, we present only that part of the transformation theory required for the local analysis of limit cycle oscillations on the center manifold of Chua's circuit.

Consider the class of nonlinear vector fields in R^3 of the form

$$\begin{bmatrix} \dot{u} \\ \dot{v} \\ \dot{\sigma} \end{bmatrix} = \begin{bmatrix} 0 & -\omega_0 & 0 \\ \omega_0 & 0 & 0 \\ 0 & 0 & 0 \end{bmatrix} \begin{bmatrix} u \\ v \\ \sigma \end{bmatrix} + \begin{bmatrix} f_c(u, v, \sigma) \\ g_c(u, v, \sigma) \\ 0 \end{bmatrix} \tag{9}$$

obtained by substituting the nonlinear graph $w = S(u, v, \sigma)$ into (6). Since the normal form computation is an iterative transformation involving terms of increasing order, we shall use the notion of k-jets to specify the terms of a specific order. The k-jet of a function $f(x)$ is denoted by $f^k(x)$ and is obtained by truncating all terms of the Taylor series expansion of degree greater than k. The notation $f_i(x)$ denotes the ith-order terms.

Using the k-jet notation, the nonlinear vector field may be represented as $\nu = \nu^{k-1} + h_k$, where ν^{k-1} is the $(k-1)$-jet of ν, and h_k contains terms of degree k or higher. The recursive algorithm for deriving the normal form of ν is based on the concept of infinitesimal deformation of the vector field. From a lemma in differential geometry [6], we know that for a vector field ν, a generator function Y satisfying the constraint

$$\left[Y^k, \nu^k\right]^{k-1} = 0 \tag{10}$$

transforms the vector field ν while leaving the $(k-1)$-jet of ν^k unchanged [6]. The Lie bracket operator $[\cdot, \cdot]$

$$[Y, \nu] = (D\nu)Y - (DY)\nu \tag{11}$$

has been used for notational convenience [17], [18], and the symbol D represents the differential operator. Under the constraint of (10), *the kth order normal form problem on H_k* is described by the differential equation [6]

$$\frac{d}{dt} h_k(\tau) = -\left[Y^k, \nu^{k-1} + h_k(\tau)\right]_k \tag{12}$$

for $h_k(\tau) \in H_k$ consisting of all homogeneous vector fields of order k, and $[Y, \nu]_k$ denotes the kth-order part of the Lie bracket operator. The solution $h_k(\tau)$ characterizes the infinitesimal deformations of the vector field; hence, the simplest normal form corresponds to the simplest solution to $h_k(\tau)$.

The Lie bracket operator is used to construct a set of basis vectors that identify a subspace B_k in H_k. The vector space can be decomposed into $H_k = B_k + G_k$, where G_k is the complementary subspace to B_k in H_k. The kth-order normal form problem in B_k can be transformed into the corresponding problem

$$\frac{d}{dt} g_k(t) = -\pi_k\left(\left[Y^{k-1}, \nu^{k-1} + g_k(t)\right]_k\right) \tag{13}$$

on the lower dimensional space G_k [6]. The map $\pi_k : H_k \to G_k$ projects the elements in H_k onto the nullspace G_k. It will be shown in the next section that this formulation of the normal form problem can be used to generate a linear system of differential equations in the normal form coefficients which can be easily solved.

2.4. Computation of the Normal Form

According to the preceding theory, the kth-order normal form problem reduces to finding a solution to (13) for some generator function Y and vector field ν. The normal form computations of Takens [13] and Ushiki [6] make coordinate transformations in the complementary space G_k in order to simplify the form of the dynamical system. Taken's method assumes that the coefficients in the transformation are fixed and then uses rescaling to simplify the normal form coefficients. In Ushiki's method, the coefficients are parameterized so that a particularly simple solution for the system of ODE's generated by (13) can be chosen for certain parameter values.

The projection of Chua's circuit onto the center manifold at $P_{\pm}$

$$\begin{bmatrix}\dot{x}\\ \dot{y}\\ \dot{z}\end{bmatrix} = \begin{bmatrix}0 & -\omega_0 & 0\\ \omega_0 & 0 & 0\\ 0 & 0 & 0\end{bmatrix}\begin{bmatrix}x\\ y\\ z\end{bmatrix} + \mathcal{O}\left(|x,y,z|^2\right) \tag{14}$$

with the variables relabeled as x, y, z has the 1-jet vector field ν_1

$$\begin{aligned}\dot{x} &= -\omega_0 y\\ \dot{y} &= \omega_0 x\\ \dot{z} &= 0\end{aligned} \tag{15}$$

on $\mathcal{R}^3$. This vector field can be conveniently represented in partial operator notation

$$\nu_1 = -y\frac{\partial}{\partial x} + x\frac{\partial}{\partial y} \tag{16}$$

where, for notational simplicity, it is assumed that $\omega_0 = 1$. The algorithm for computing the normal form follows.

Step 1: Construct the Basis for H_k: The vector space H_k of homogeneous vector fields of degree k is determined from the linear map

$$L_k : Y_k \in H_k \rightarrow [Y_k, \nu_1] \in H_k \tag{17}$$

applied to the vector field ν_1 and the basis of homogeneous polynomials

$$Y_k = \left\{x_l y_m z_n\frac{\partial}{\partial x}, x_l y_m z_n\frac{\partial}{\partial y}, x_l y_m z_n\frac{\partial}{\partial z}\right\} \quad l+m+n=k. \tag{18}$$

For the second-order normal form problem, the basis for H_2 consists of 18 monomials

$$Y_2 = \left\{\begin{array}{l} x^2\frac{\partial}{\partial x}, xy\frac{\partial}{\partial x}, y^2\frac{\partial}{\partial x}, xz\frac{\partial}{\partial x}, yz\frac{\partial}{\partial x}, z^2\frac{\partial}{\partial x},\\ x^2\frac{\partial}{\partial y}, xy\frac{\partial}{\partial y}, y^2\frac{\partial}{\partial y}, xz\frac{\partial}{\partial y}, yz\frac{\partial}{\partial y}, z^2\frac{\partial}{\partial y},\\ x^2\frac{\partial}{\partial z}, xy\frac{\partial}{\partial z}, y^2\frac{\partial}{\partial z}, xz\frac{\partial}{\partial z}, yz\frac{\partial}{\partial z}, z^2\frac{\partial}{\partial z}\end{array}\right\} \tag{19}$$

expressed in partial operator notation. The linear map L_2 may be represented in matrix form in which the ith column contains the coefficients of the linear map L_2 applied to ν_1 and the ith basis vector in Y_2. The subspace B_2 consists of all elements of the form $[Y_2, \nu_1] \in H_2$. For example, the map L_2 applied to the three monomials $xy\frac{\partial}{\partial x}$, $xy\frac{\partial}{\partial y}$, and $xy\frac{\partial}{\partial z}$ in Y_2 yields

$$\begin{aligned}\left[xy\frac{\partial}{\partial x}, \nu_1\right] &= (-x^2+y^2)\frac{\partial}{\partial x} - xy\frac{\partial}{\partial y}\\ \left[xy\frac{\partial}{\partial y}, \nu_1\right] &= -xy\frac{\partial}{\partial x} + (-x^2+y^2)\frac{\partial}{\partial y}\\ \left[xy\frac{\partial}{\partial z}, \nu_1\right] &= (-x^2+y^2)\frac{\partial}{\partial z}.\end{aligned} \tag{20}$$

Continuing in this way for all elements of Y_2, the linear map for L_2 can be represented by the matrix

$$M_2 = \begin{bmatrix}A & -I & 0\\ I & A & 0\\ 0 & 0 & A\end{bmatrix} \tag{21}$$

where I denotes a 6×6 identity matrix, and

$$A = \begin{bmatrix}0 & -1 & 0 & 0 & 0 & 0\\ 2 & 0 & -2 & 0 & 0 & 0\\ 0 & 1 & 0 & 0 & 0 & 0\\ 0 & 0 & 0 & 0 & -1 & 0\\ 0 & 0 & 0 & 1 & 0 & 0\\ 0 & 0 & 0 & 0 & 0 & 0\end{bmatrix} \tag{22}$$

where each partition in M_2 is indexed according to the set of monomials $\{x^2, xy, y^2, xz, yz, z^2\}$. The basis vectors B_2 for the second-order normal form are determined from the column space of M_2. The rank of M_2 is 14, and therefore, the nullspace G_2 is given by a linear combination of four vectors that can be represented in partial operator notation as

$$\begin{aligned}g_2(\tau) =& a_1(\tau)\left(xz\frac{\partial}{\partial x} + yz\frac{\partial}{\partial y}\right) + a_2(\tau)\left(-yz\frac{\partial}{\partial x} + xz\frac{\partial}{\partial y}\right)\\ &+ b_1(\tau)\left((x^2+y^2)\frac{\partial}{\partial z}\right) + b_2(\tau)\left(z^2\frac{\partial}{\partial z}\right)\end{aligned} \tag{23}$$

where the coefficients a_i and b_i depend continuously on the parameter τ.

Step 2: Determine the Form of the Generator Y_k: The generator function Y^{k-1} in (13) is assumed to be a linear combination of homogeneous polynomials in $\{x, y, z\}$. The invariance constraint of (10) can be applied to determine the specific form of Y. If we let

$$\begin{aligned}Y_1 =& (A_1x + A_2y + A_3z)\frac{\partial}{\partial x}\\ &+ (B_1x + B_2y + B_3z)\frac{\partial}{\partial y}\\ &+ (C_1x + C_2y + C_3z)\frac{\partial}{\partial z}\end{aligned} \tag{24}$$

then applying the constraint equation using ν_1 in (16) yields

$$\begin{aligned}A_1 &= B_2\\ A_2 &= -B_1\\ A_3 &= B_3 = C_1 = C_2 = 0\end{aligned} \tag{25}$$

and the value of C_3 is unconstrained. Consequently, Y_1 must assume the form

$$Y_1 = \alpha\left(x\frac{\partial}{\partial x} + y\frac{\partial}{\partial y}\right) + \beta\left(y\frac{\partial}{\partial x} - x\frac{\partial}{\partial y}\right) + \gamma\left(z\frac{\partial}{\partial z}\right) \tag{26}$$

where we have renamed $A_1 = \alpha$, $A_2 = \beta$, and $C_3 = \gamma$.

Step 3: Solve for the Normal-Form Coefficients: Since the projection mapping is $\pi_2 : H_2 \rightarrow G_2$, it follows that $\pi_2(b) = 0$ for any $b \in B_2$. Therefore, the right-hand side of

$$\frac{d}{d\tau} g_2(\tau) = -\pi_2([Y_1, g_2(\tau)]_k) \tag{27}$$

reduces to

$$\begin{aligned} -\pi_2([Y_1, g_2(\tau)]_2) &= \gamma a_1(\tau)\left(xz\frac{\partial}{\partial x} - yz\frac{\partial}{\partial y}\right) \\ &+ \gamma a_2(\tau)\left(-yz\frac{\partial}{\partial x} + xz\frac{\partial}{\partial y}\right) \\ &+ (2\alpha - \gamma) b_1(\tau)\left((x^2+y^2)\frac{\partial}{\partial z}\right) + \gamma b_2(\tau)\left(z^2\frac{\partial}{\partial z}\right) \end{aligned} \tag{28}$$

Matching coefficients from (27) using the projection (28) yields the linear system of ordinary differential equations

$$\begin{aligned} \dot{a_1} &= \gamma a_1 \\ \dot{a_2} &= \gamma a_2 \\ \dot{b_1} &= (2\alpha - \gamma) b_1 \\ \dot{b_2} &= \gamma b_2 \end{aligned} \tag{29}$$

with solutions

$$\begin{aligned} a_1(\tau) &= a_1(0)e^{\gamma\tau} \\ a_2(\tau) &= a_2(0)e^{\gamma\tau} \\ b_1(\tau) &= b_1(0)e^{(2\alpha-\gamma)\tau} \\ b_2(\tau) &= b_2(0)e^{\gamma\tau}. \end{aligned} \tag{30}$$

If $a_1(0) \neq 0$, then we can choose $\gamma = \log|a_1(0)|$ so that at $\tau = 1$, we have $a_1(1) = a_1(0)e^{\gamma}$; thus, $a_1(1) = \pm 1$. Furthermore, if we choose $\alpha = \frac{1}{2}(\log|a_1(0)| - \log|b_1(0)|)$, then $b_1(1) = \pm 1$.

The second-order normal form is obtained by evaluating $g_2(\tau)$ in (23) at $\tau = 1$. Combining linear terms from (14) with $g_2(1)$ gives

$$\begin{bmatrix} \dot{x} \\ \dot{y} \\ \dot{z} \end{bmatrix} = \begin{bmatrix} 0 & -\omega_0 & 0 \\ \omega_0 & 0 & 0 \\ 0 & 0 & 0 \end{bmatrix} \begin{bmatrix} x \\ y \\ z \end{bmatrix} + \begin{bmatrix} s_1 xz - a_2 yz \\ a_2 xz + s_1 yz \\ s_2(x^2+y^2) + b_2 z^2 \end{bmatrix} \tag{31}$$

as the second-order normal form, where $s_1 = \pm 1$ and $s_2 = \pm 1$.

Once the second-order terms have been converted to normal form, the same methods can be applied to derive the third-order terms. The third-order normal form on the center manifold is given by

$$\begin{bmatrix} \dot{x} \\ \dot{y} \\ \dot{z} \end{bmatrix} = \begin{bmatrix} 0 & -\omega_0 & 0 \\ \omega_0 & 0 & 0 \\ 0 & 0 & 0 \end{bmatrix} \begin{bmatrix} x \\ y \\ z \end{bmatrix} + \begin{bmatrix} s_1 xz - a_2 yz \\ a_2 xz + s_1 yz \\ s_2(x^2+y^2) + b_2 z^2 \end{bmatrix} + \begin{bmatrix} a_3(x^2+y^2)x - a_4(x^2+y^2)y \\ a_4(x^2+y^2)x + a_3(x^2+y^2)y \\ b_4 z^3 \end{bmatrix}. \tag{32}$$

This normal form has a particularly simple form when expressed in cylindrical polar coordinates

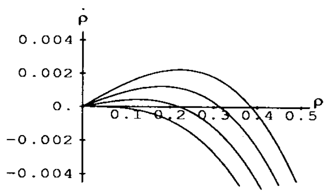

Fig. 4. One-dimensional bifurcation function in which the zeros indicate the amplitude of stable limit cycles. The parameter values are $\alpha = 6.6$, $\beta = 14.0$, and $\sigma = 0,\ 0.05,\ 0.1,\ 0.015$.

$$\dot{\rho} = s_1 \rho z + a_3 \rho^3 + \mathcal{O}\left(|\rho, \theta, z|^4\right) \tag{33a}$$

$$\dot{\theta} = \omega_0 + a_2 z + a_4 \rho^2 + \mathcal{O}\left(|\rho, \theta, z|^4\right) \tag{33b}$$

$$\dot{z} = s_2 \rho^2 + b_2 z^2 + b_4 z^3 + \mathcal{O}\left(|\rho, \theta, z|^4\right) \tag{33c}$$

evaluated up to order three. When applied to the analysis of limit cycle behavior in Chua's circuit, the value of ρ corresponds to the radius of the limit cycle on the uv surface of the center manifold, θ is the phase angle between the u and v coordinates, and z corresponds to the bifurcation parameter σ in the augmented system in (6).

III. Bifurcation Function

One purpose for computing the normal form equation for Chua's circuit is to derive a reduced order *bifurcation function* which characterizes the amplitude of the structurally stable limit cycle oscillations [13], [16], [19]. Our goal is to understand the local behavior of Chua's circuit on the 2-D center manifold. The Hopf bifurcation curve

$$\beta = \frac{2}{9}\alpha(3+\alpha) \tag{34}$$

specifies the values of the parameters α and β of (1) at which periodic oscillations emerge from a stable fixed point [2]. The 1-D equation in ρ in (33a) describes the amplitude of the limit cycle oscillations in the neighborhood of the Hopf bifurcation curve. For small values of σ and ρ, the bifurcation function

$$\dot{\rho} = \sigma\rho + a_3\rho^3 \tag{35}$$

shows that the amplitude of limit cycle oscillations varies with σ and has the stable amplitude $\rho_0 = \sqrt{\frac{-\sigma}{a_3}}$. As the parameter σ increases through zero (e.g., by increasing values of α with β fixed), a Hopf bifurcation from the fixed point to a limit cycle occurs [13].

The shape of the bifurcation function in (35) is shown in Fig. 4 for the case $\alpha = 6.6$, $\beta = 14.0$, and σ is small. Since the value of ρ is interpreted as the amplitude of the oscillations, we shall consider only zeros in the right half plane of Fig. 4. In this case, there are two zeros for each bifurcation curve. The zero at the origin with $\rho = 0$ is unstable, and hence, any trajectory starting near the origin will expand outward. The zero at $\rho_0 \neq 0$ is stable and determines the amplitude of the stable limit cycle on the center manifold.

In the case where σ is not small, it is necessary to rederive the bifurcation function from the normal form. Closed-form expressions for the normal form coefficients in terms of the dynamics on the center manifold enable the direct computation of the bifurcation function. The computation of the normal form was based on successive transformations that simplify terms of order k without modifying lower order terms. However, terms of order higher than k are modified by each transformation. In order to calculate the coefficients for each term of the normal form in terms of the original vector field, it is necessary to keep track of all modifications to the higher order terms for each successive transformation.

The general form of the dynamics projected onto the center manifold is given by

$$\begin{bmatrix} \dot{u} \\ \dot{v} \\ \dot{\sigma} \end{bmatrix} = \begin{bmatrix} 0 & \omega_0 & 0 \\ \omega_0 & 0 & 0 \\ 0 & 0 & 0 \end{bmatrix} \begin{bmatrix} u \\ v \\ \sigma \end{bmatrix} + \begin{bmatrix} \sigma u \\ \sigma v \\ 0 \end{bmatrix} + \begin{bmatrix} f_c(u,v) \\ g_c(u,v) \\ h_c(u,v) \end{bmatrix} \tag{36}$$

where σ is considered as a constant. The procedure for computing the values of the normal form coefficients in terms of the vector field in (36) is detailed in [13]. The resultant coefficients a_i in (32) are given by (37), which is shown at the botom of this page, where the expansion has been evaluated up to third order. The expressions in (37) provide a closed-form solution for the coefficients for the Ushiki normal form. The value of the coefficient a_3 in the bifurcation function (35) can be obtained directly from (37).

In Fig. 4, the value of σ was nearly zero, and the slope of the bifurcation function at the zero of the function was nearly parallel to the σ axis. Thus, the rate of convergence onto the limit cycle is slow, and the amplitude of the limit cycle oscillations will be strongly influenced by noise, variation of initial conditions, and interactions with spatially coupled systems. As the value of α increases toward $\alpha = 7.4$ in Fig. 5(a) (and hence σ increases), the zero crossing of the bifurcation function and the slope increase as shown in Fig. 5(b). Hence, the parameter σ predicts the occurrence of a Hopf bifurcation, and the slope of the bifurcation function through the zero crossing provides a useful measure of limit cycle stability.

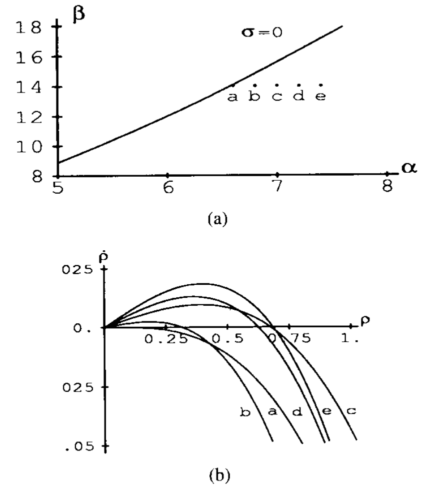

Fig. 5. Partial bifurcation diagram of Chua's circuit. (a) Hopf bifurcation curve in the $\alpha\beta$-space. (b) Bifurcation functions along $\beta = 14.0$ for point a, $(\alpha, \sigma) = (6.6, 0.0)$; point b, $(6.8, 0.002)$; point c, $(7.0, 0.037)$; point d, $(7.2, 0.054)$; point e, $(7.4, 0.070)$.

IV. Application to Gesture Recognition

In this section, preliminary results for an array of Chua's circuits for hand gesture recognition are described. Hand gestures in American sign language (ASL) are characterized in terms of i) the region of articulation in physical space, ii) the trajectory of the hand motion, and iii) the hand configuration as a function of position along the motion trajectory [20]. Many gestures in ASL employ a fixed hand configuration along the hand motion trajectory, and therefore, the focus of this paper concerns only the identification of the place of articulation and the recognition of the motion trajectory. The recognition of hand shape is to be performed by a separate module. A restricted set of trajectories consisting of circular motions in various regions and orientations in the physical space are examined. This initial set of trajectories is chosen to allow the direct mapping between the space coordinates of the input trajectory and the xyz variables of Chua's circuit equations.

$$\begin{aligned}
a_2 &= -\frac{1}{2}(f_{011} - g_{101}) \\
a_3 &= \frac{1}{16}(g_{030} + f_{120} + g_{210} + f_{300}) + \\
&\quad \frac{1}{16\omega_0}(f_{020}g_{020} + f_{020}f_{110} - g_{020}g_{110} + f_{110}f_{200} - g_{110}g_{200} - f_{200}g_{200}) \\
a_4 &= \frac{1}{16}(-f_{030} + g_{120} - f_{210} + g_{300}) + \\
&\quad \frac{1}{48\omega_0}(-5f_{020}^2 - 2g_{020}^2 + 5f_{110}g_{020} - 2f_{110}^2 + f_{020}g_{110} - 2g_{110}^2 - \\
&\quad 5f_{020}f_{200} + 5f_{200}g_{110} - 5g_{020}g_{200} + f_{110}g_{200} - 5g_{200}^2 - 2f_{200}^2) \\
b_2 &= \frac{1}{4}(h_{200} + h_{020}) \\
b_4 &= \frac{1}{2}h_{002}
\end{aligned} \tag{37}$$

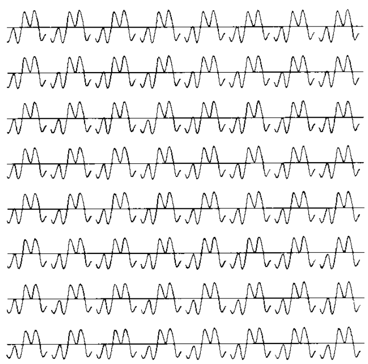

Fig. 6. Synchrony of the x component for an 8×8 array of Chua's circuits driven by a nonperiodic function.

The dynamics of an array of Chua's circuits are made as simple as possible in order to illustrate the global entrainment of the array and the subsequent formation of spatial patterns for recognition. Reshaping the trajectories on the center manifold surface using the normal form theory is not included in this illustration.

The thorough development of nonlinear oscillators for trajectory recognition depends on the elaboration of the transformational theory on the center manifold. The analysis of the previous sections provides a description for the behavior of limit cycle oscillations of an autonomous Chua's circuit near the center manifold surface. Since chaotic trajectories emerge from the limit cycle trajectories as the bifurcation parameter is increased, this analysis applies to a wide range of nonlinear oscillations on the center manifold.

The initial design of the recognition system consists of an array of Chua's circuits in which each system in the array is rotated along the horizontal and vertical directions so that the center manifold is approximately aligned with one of the trajectories from the restricted set of gestures. The driven form of Chua's circuit is

$$\begin{aligned} \dot{x} &= \alpha[y - f(x)] \\ \dot{y} &= x - y + z + g(t) \\ \dot{z} &= -\beta y \end{aligned} \tag{38}$$

where the function $g(t)$ provides the input trajectory to the circuit. The driving function is $g(t) = \gamma(h_x(t) - x)$, where γ is the coupling coefficient, and $h_x(t)$ corresponds to the x-projection of the 3-D hand motion trajectory to be recognized. Each element in the array contains a rotated version of (38) in order to illustrate the properties of synchronization and pattern formation.

The interpretation of the state of the nonlinear oscillator may be as difficult to achieve as the original recognition task. This problem is greatly simplified by the entrainment of the nonlinear oscillator to the input trajectory. The perturbation to the dynamics in (38) is minimized when $x = h_x(t)$, thus leading to the entrainment of the x component to the input. The global entrainment of the array is illustrated in Fig. 6 with an 8×8 array of Chua's circuits with rotated center manifolds.

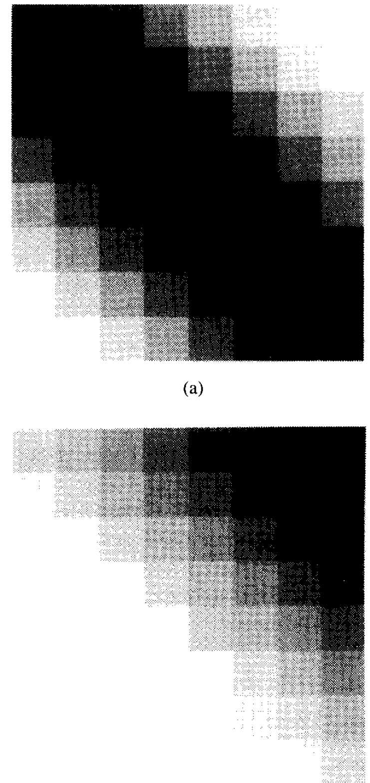

(a)

(b)

Fig. 7. Spatial patterns created in an array of Chua's circuits driven by two different trajectories. Brightness indicates distance from the center manifold. (a) Input is close to the manifolds of the diagonal elements, and (b) input is close to the manifolds of the upper right elements.

The trajectories on the center manifold provide a representation for the class of trajectories to be recognized. The entrainment of the x component provides the temporal alignment with the input trajectory. The distance between the center manifold surface and the y and z components of the input provide a measure for the quality of the match between the class of trajectories on the manifold surface and the 3-D input trajectory. Chua's circuit with α and β chosen to produce chaotic oscillations ensures rapid convergence onto the center manifold surface, and therefore, the Euclidean distance $\left((h_x - x_{ij})^2 + (h_y - y_{ij})^2 + (h_z - z_{ij})^2\right)^{\frac{1}{2}}$ provides a simple measure for the quality of match between trajectories. Fig. 7 shows two spatial patterns obtained by evaluating this distance measure for two input trajectories to the array. Note that the inclusion of the x component in the distance measure means that the distance is small when there is entrainment and the input trajectory is near the center manifold surface.

The initial design of the array is based upon the assumption of closed, circular orbits in a plane. The synchronization of all circuits in the array and the formation of spatial patterns were shown for this simple case. The recognition of more complex trajectories on a non-planar surface can be accomplished by modifying the center manifold surface of the dynamical systems. According to the nonlinear transformation theory developed in the previous sections, the shape of the center manifold surface can be modified using (7). The perturbation of the original dynamics by the new center manifold is obtained from (8) followed by the inverse Jordan transformation. Furthermore, the normal form of the modified dynamics is computed directly from the center manifold using the expressions for the coefficients in (37).

V. Conclusion

A paradigm for the study of nonlinear systems has recently emerged with the introduction of Chua's circuit and its associated canonical circuit family. The relative simplicity of Chua's circuit provides a convenient model of the dynamics and bifurcation phenomena for the design of more complex systems. A critical step in the design process is the representation of the dynamics on the center manifold. In this paper, the normal form method of Ushiki has been used to determine a bifurcation function. Closed-form solutions were derived for the normal form coefficients for Chua's circuit with a cubic nonlinearity. A simple application of an array of Chua's circuits used as nonlinear oscillators for trajectory recognition was illustrated.

References

[1] L. O. Chua, "Global unfolding of Chua's circuit," *IEICE Trans. Fundamentals*, vol. E76-A, pp. 704–734, May 1993.
[2] A. I. Khibnik, D. Rose, and L. O. Chua, "On periodic orbits and homoclinic bifurcations in Chua's circuit with smooth nonlinearity," *Int. J. Bifurcation Chaos*, vol. 3, Apr. 1993.
[3] R. N. Madan (Guest Editor), Special issue on "Chua's circuit: A paradigm for chaos," *J.Circuits Syst. Comput.*, vol. 3, nos. 1 and 2, 1993.
[4] M. Delgado-Restituto and A. Rodriguez-Vazquez, "A CMOS monolithic Chua's circuit," in *Chua's Circuit: A Paradigm for Chaos* (R. N. Madan, Ed.). Singapore: World Scientific, 1993.
[5] S. Ushiki, "Normal forms for singularities of vector fields," *Japan J. Appl. Math*, vol. 1, pp. 1–37, 1984.
[6] L. O. Chua and H. Kokubu, "Normal forms for nonlinear vector fields–Part I: Theory and algorithm," *IEEE Trans. Circuits Syst.*, vol. 35, no. 7, pp. 863–880, 1988.
[7] L. O. Chua and H. Kokubu, "Normal forms for nonlinear vector fields—Part II: Applications," *IEEE Trans. Circuits Syst.*, vol. 36, no. 8, pp. 51–70, 1989.
[8] T. Matsumoto, L. O. Chua, and M. Komuro, "The double scroll," *IEEE Trans. Circuits Syst.*, vol. 32, pp. 797–818, 1985.
[9] L. O. Chua, "Nonlinear circuits," *IEEE Trans. Circuits Syst.*, vol. 31, no. 1, pp. 69–87, 1984.
[10] L. O. Chua, M. Komuro, and T. Matsumoto, "The double scroll family," *IEEE Trans. Circuits Syst.*, vol. 33, no. 11, pp. 1073–1118, 1986.
[11] M. P. Kennedy, "Robust op amp realization of Chua's circuit," *Frequenz*, vol. 46, no. 34, pp. 66–80, 1992.
[12] M. W. Hirsch and S. Smale, *Differential Equations, Dynamical Systems and Linear Algebra*. New York, NY: Academic, 1974.
[13] J. Guckenheimer and P. Holmes, *Nonlinear Oscillations, Dynamical Systems, and Bifurcations of Vector Fields*. New York: Springer-Verlag, 1983.
[14] J. Carr, *Applications of Center Manifold Theory*. New York: Springer-Verlag, 1981.
[15] S. Wiggins, *Introduction to Applied Nonlinear Dynamical Systems and Chaos*. New York: Springer-Verlag, 1990.
[16] E. J. Altman, "Bifurcation analysis of Chua's circuit with applications for low-level visual sensing," *J. Circuits Syst. Comput.*, vol. 3, no. 1, pp. 63–92, 1993.
[17] R. H. Abraham and J. E. Marsden, *Foundations of Mechanics*. Reading, MA: Benjamin/Commings, 1978.
[18] Y. Choquet-Bruhat, C. Dewitt-Morett, and M. Dillard-Bleick, *Analysis Manifolds and Physics*. Amsterdam: North Holland, 1977.
[19] S. N. Chow and J. K. Hale, *Methods of Bifurcation Theory*. New York: Springer-Verlag, 1982.
[20] H. Poizner, E. S. Klima, and U. Bellugi, *What the Hands Reveal about the Brain*. Cambridge, MA: MIT Press, 1987.

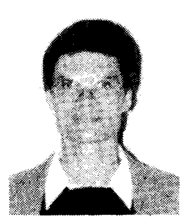

Edward J. Altman received the Bachelor's degree in electrical engineering from Rose-Hulman Institute of Technology, Terre Haute, IN, in 1978. He received the Master's and Ph.D. degrees in electrical engineering from the University of Illinois at Urbana-Champaign in 1984 and 1991, respectively. He held a post doctoral research position in computer vision with the Beckman Institute at the University of Illinois until 1992.

Currently, he is a visiting researcher at ATR Communication Systems Research Laboratory in Kyoto, Japan. His research interests include nonlinear dynamical systems and hand gesture recognition with an emphasis on sign language interpretation and human-computer interaction.